

EXCESS ENTHALPIES OF LIQUID MIXTURES AT HIGH PRESSURE.
EXPERIMENTAL TECHNIQUES AND MOLECULAR INTERPRETATION

A. Heintz and R.N. Lichtenthaler

Physikalisch-Chemisches Institut der Universität
Heidelberg / West Germany

ABSTRACT

Calorimetric equipment and experimental procedures recently developed for measuring excess enthalpies of liquid mixtures at high pressures are described. Experimental results of alkane-alkane mixtures and alcohol-alkane mixtures are discussed according to the Prigogine-Flory free volume theory and the real associated solution model.

INTRODUCTION

The interest in experimental and theoretical work on thermodynamic properties of liquid mixtures has increased within the last years. Most of this work has been done in the field of fluid phase equilibria but also excess properties in the liquid and supercritical region have been measured which partly indicate a remarkable change with increasing pressure. Mainly data of the excess volume V^E have been determined (ref. 1-8) and until about three years ago only some data of the excess enthalpy H^E at high pressure existed (ref. 9-13). In the meantime, however, a few high-pressure-flow calorimeters have been developed suitable for measurements of endothermic and exothermic excess enthalpies (ref. 14-16).

Nowadays it is therefore possible to determine excess properties experimentally over a wide range of pressure and temperature with such a precision that systematic investigations of these properties allow to study the thermodynamic behavior of fluids and their mixtures.

From the theoretical point of view excess properties at high pressure are of particular interest. High pressure thermodynamic behavior of fluids and their mixtures sensitively depends on the intermolecular interactions especially on the repulsive forces. Therefore, data of excess properties at high pressures provide an important test of current molecular theories, e.g. perturbation theories or modern free volume theories.

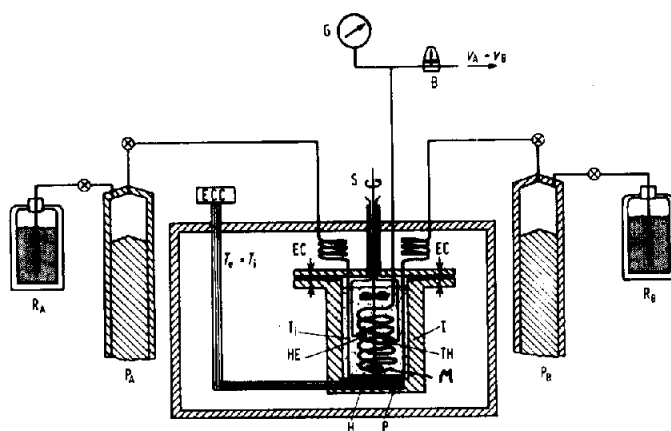
In the first section of this article a description of calorimetric experimental equipment is given which has proved to provide reliable results working at pressures higher than 100 bar. The principle of flow calorimetry is the common constructive feature of all calorimeters described. This calorimetric method presents not only an elegant procedure of measuring excess enthalpies of fluid mixtures at high pressure but also is the easiest way of avoiding vapor space in the liquid system which is an indispensable precondition at working with liquids under high pressure.

In the second and third sections experimental results and theoretical interpretations of two groups of binary systems are presented and discussed: alkane-alkane mixtures and alkane-alcohol mixtures.

HIGH PRESSURE CALORIMETRIC PROCEDURES

Fig. 1 shows the schematic diagram of the isothermal flow calorimeter originally published by Heintz et al. (ref. 14).

The reaction vessel (1) containing the internal waterbath of the temperature T , has a volume of about 30 ml. It is immersed in a large external waterbath (~ 100 l) whose temperature $T_e = T_i$ is controlled to within $\pm 10^{-3}$ K. To measure the enthalpy of mixing,



P_A, P_B	High pressure pumps	TH	Control thermistor
R_A, R_B	Liquid reservoirs	H	Control heater
⊗	High pressure valves	P	Peltier cooler
G	High pressure gauge	HE	Calibration heater
B	Back pressure regulator	EC	Equilibrating coils
I	Insulated reaction vessel	M	Beginning of mixing coil
T_c	Temperature in the external water bath	S	Stirrer
T_i	Temperature in the reaction vessel	ECC	Electronic control circuit

Fig. 1. Schematics of high pressure flow calorimeter.

the two liquid components A and B are pumped through equilibrating coils (EC) in the outer waterbath and enter at point M into the mixing coil in the internal waterbath. For all coils stainless steel tubing is used (wall thickness = 0.3 mm, internal diameter = 0.9 mm). The energy liberated (exothermic) or absorbed (endothermic) during mixing is absorbed or delivered by the water in the reaction vessel. A Peltier cooler at the bottom of the reaction vessel removes energy from the water inside at a constant rate and discharges it to the surrounding waterbath. A controlled heater (Electronic Control Circuit Tronac 1250) compensates for this energy and for the energy liberated or absorbed by the mixing process maintaining the internal waterbath at a constant temperature (to within $\pm 2 \cdot 10^{-5}$ K). The difference in the energy supplied by the heater during and before

a mixing process is a direct measure of the energy of mixing. The number of heat pulses (0 - 25.000/sec) supplied to the heater are counted and registered. The temperature T_i is controlled with a thermistor (TH) and a stirrer (S) assures a homogeneous temperature within the bath. Using the heater HE, a well defined energy can be generated thus making the calibration of the whole system possible.

Two high pressure pumps (P_A, P_B ; Varian HPLC 8500) coupled with a back pressure regulating valve (B; Circle Seal Corp.) allow the unit to be run at any pressure from 1 to 600 bar. Pressures are measured with a precision Heise gauge (G) whose accuracy is 0.1% of full scale (± 1 bar). The flow rates of the two pumps are independent of pressures and can be varied in steps of 1 ml/h to formulate mixtures of different compositions in the mixing coil. The flow rates must not be chosen too high to assure complete heat exchange before the mixtures leave the mixing coil.

Knowing the volumetric flow rates \dot{v}_A and \dot{v}_B delivered by the two pumps the molar excess enthalpy H^E is given by:

$$H^E = \frac{q_M}{\dot{v}_A \frac{\rho_A}{M_A} + \dot{v}_B \frac{\rho_B}{M_B}} \quad (1)$$

where q_M is the change in the heating power before and during the continuous mixing process; ρ_A and ρ_B are the densities of the two components at the pressure and temperature under investigation; and M_A and M_B are the molar masses. The mole fraction of the mixture obtained in the mixing coil is:

$$x_A = \frac{\dot{v}_A \frac{\rho_A}{M_A}}{\dot{v}_A \frac{\rho_A}{M_A} + \dot{v}_B \frac{\rho_B}{M_B}} \quad (2)$$

The mixing coil is about 45 cm long and has a volume of about 1 ml. Measurements have been performed with different \dot{v}_A and \dot{v}_B but with a constant ratio \dot{v}_A/\dot{v}_B for each system to find the limiting flow

consistent with complete heat exchange.

As an example of the experimental procedure, Fig. 2 shows the analog registration of the heating power necessary to keep the system isothermal at 1 bar and at 300 bar, respectively. The measurement was performed with $n\text{-C}_6 + c\text{-C}_6$ at a mole fraction $x_{n\text{-C}_6} = 0.453$ and at 298.15 K. The change q_M of the heating power with respect to the baseline corresponds to the change in the heat pulse rate supplied to the control heater before and during mixing. There are two reasons for the different values of q_M at 1 bar and at 300 bar. The endothermic H^E is larger at 300 bar and the molar flow at 300 bar is larger, too, due to the increase in density. To determine q_M , the heat pulse rate is measured and registered at intervals of 1 minute each. The difference in the time-averaged heat pulse rates before and during mixing gives q_M directly after calibration of the system has been performed.

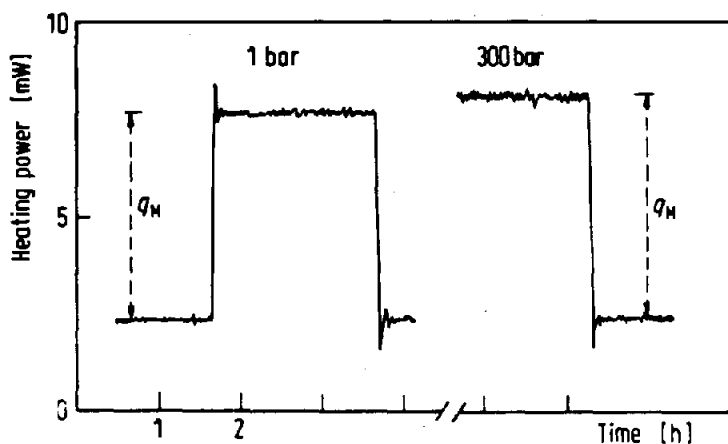


Fig. 2. Analog registration for $n\text{-C}_6 + c\text{-C}_6$ with $x_{n\text{-C}_6} = 0.453$ at 298.15 K and 1 and 300 bar.

A similar high pressure calorimeter has been constructed by Christensen et al. (ref. 12) and its recent modification (ref. 15) is shown in Fig. 3. Instead of the external waterbath an air bath is used in which the reaction vessel, thermal shields, and accompanying supply lines are suspended. The air bath is capable of

temperature control to better than ± 1 K over the temperature range 253 to 473 K. The isothermal electronic control system is the same as in the calorimeter described above (see also Fig. 1) but the construction of the reaction vessel is different. The brass reaction vessel (Fig. 3) contains an isothermal plate and equilibrium coil.

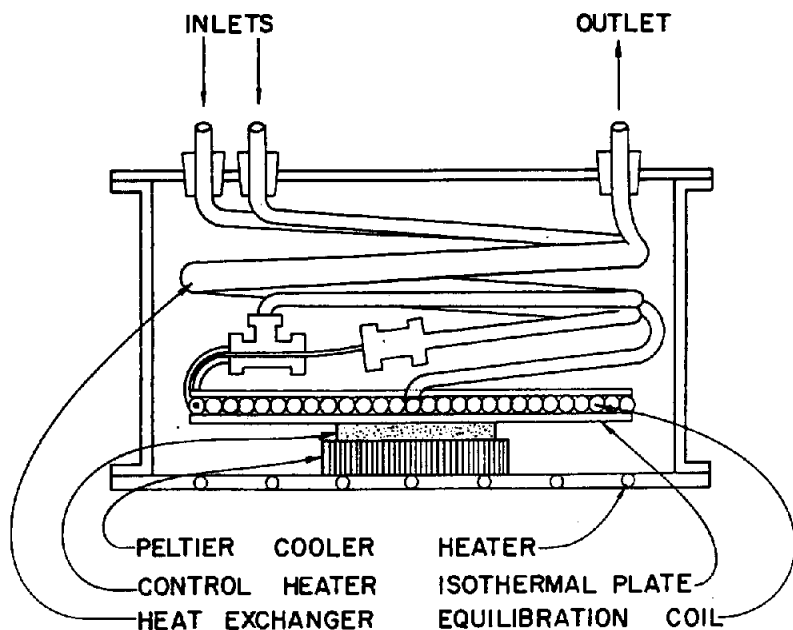


Fig. 3. Reaction vessel with isothermal plate according to Christensen et al. (ref. 15).

Under the plate are a 100 ohm wafer control heater and a high temperature model Peltier thermoelectric cooler. The isothermal plate consists of two round brass plates with the equilibration coil soldered between the plates. After entering the reaction vessel and before entering the coil the reactants are equilibrated with the products from the coil in a countercurrent heat exchanger. The two tubes containing the reactants are brought together as shown in Fig. 4. The smaller tube is fitted inside the larger tube and the two reactant streams run coaxially for approximately 1 turn of

the equilibration coil before the smaller inlet tube ends and mixing begins. Thermistors are used to continuously monitor the reaction vessel temperature and to control the plate at a constant temperature. A 100 ohm calibration heater was placed between the tubing turns of the equilibration coil and soldered in position. The temperature of the bottom of the reaction vessel in contact with the Peltier cooler is controlled to ± 0.0005 K. The upper temperature at which the calorimeter can be operated (423 K) is limited by the Peltier cooler. It is anticipated that the upper range of the calorimeter will be extended to 470 - 480 K as Peltier coolers having higher operating temperature limits become available.

The thermal shields (not shown in Fig. 3) consist of two cans surrounding the reaction vessel. The temperature of the inner shield is controlled to ± 0.005 K. The outer shield (an aluminium can) is not temperature controlled but is allowed to assume a steady state temperature between that of the inner shield and the air bath.

The upper pressure limit of this calorimeter is 400 bar.

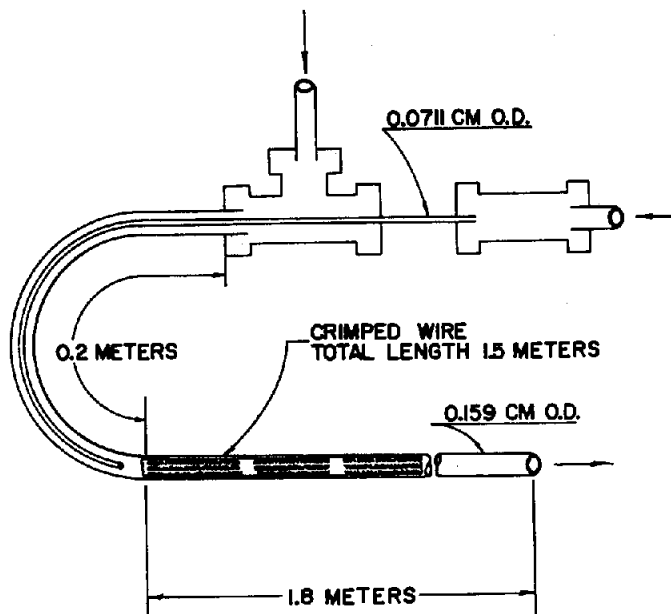


Fig. 4. Mixing procedure of the two fluid components in the reaction vessel according to Christensen et al. (ref. 15).

The principal design of the flow circuit, the high pressure pumps, and the pressure control are essentially the same as in the calorimeter of Heintz and Lichtenthaler (ref. 14). Two advantages of Christensen's calorimeter should be mentioned. Firstly, the length of the mixing coil (180 cm) allows working with relatively high volume speeds and therefore a large heat effect can be measured with the same precision as for smaller flow rates. Secondly, the air bath construction makes it possible to extend calorimetric measurements to higher temperatures. In spite of these interesting improvements only heats of mixing below 50 bar have been published so far with this apparatus (ref. 15).

Another construction of a high pressure calorimeter has been published recently by Siddiqi and Lucas (ref. 16). This apparatus is essentially identical with the calorimeter of Heintz and Lichtenthaler. A comparison of results obtained by the three calorimeters described in this section is shown in Fig. 5 for the pressure dependence of the excess enthalpy of the system $c\text{-C}_6 + n\text{-C}_6$. The agreement of the results obtained with the calorimeter by Heintz et al. and the one by Siddiqi et al. is excellent. The results obtained with Christensen's calorimeter (ref. 12) are slightly higher but still in the experimental error limits.

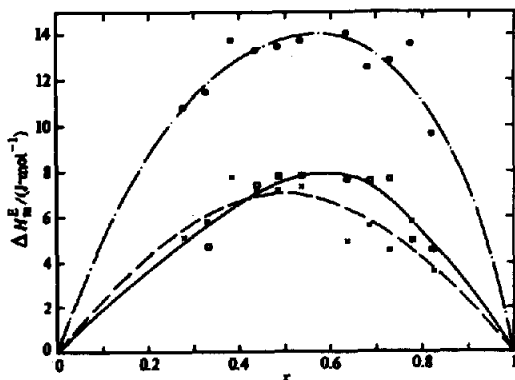


Fig. 5. Comparison of $\Delta H_m^E = H_m^E (150 \text{ bar}) - H_m^E (1 \text{ bar})$ at 298.15 K

□, ———, ΔH^E from Heintz et al. (ref. 14); -.-.-, ○, ΔH^E from Christensen et al. (ref. 12), - - - - ΔH^E representing experimental data (x) from Siddiqi et al. (ref. 16).

ALKANE + ALKANE MIXTURES

Experimental Results

At ambient pressure H^E -data for a large number of mixtures of saturated hydrocarbons at various temperatures are available (ref. 17). At high pressures systematic measurements so far have only been performed by Heintz et al. (ref. 18) and the results obtained for some mixtures are shown in Figs. 6 - 8.

The H^E -values are always positive (endothermic mixing). Either the differences

$$\Delta H^E(p) = H^E(p) - H^E(p = 1 \text{ bar}) \quad (3)$$

or the $H^E(p)$ -values directly are shown over the entire range of mole fraction x at 298.15 K. Except for the system cyclohexane (c-C₆) + 2,2,4-trimethylpentane (i-C₈), for all systems a positive value ($\Delta H^E/\Delta p$) is obtained. For the systems with c-C₆ the dependence of H^E on pressure increases with increasing chainlength of the n-alkane, i.e. with increasing differences in molecular size and shape, as shown in Figs. 6 and 7 for n-octane (n-C₈) and n-dodecane (n-C₁₂) respectively. As expected ΔH^E is relatively small, for an equimolar mixture always about 5 - 8% of the corresponding absolute H^E -values at 1 bar for an increase in pressure of 300 bar. For the systems with n-hexane (n-C₆) the absolute increase of H^E with pressure is of the same magnitude as for the corresponding mixtures with c-C₆, however, the relative change with respect to the value at 1 bar is very large, as shown in Fig. 8 for the mixture with n-decane (n-C₁₀). In all cases ($\Delta H^E/\Delta p$) decreases with increasing pressure, which was to be expected as the compressibility

of the liquids decreases with increasing pressure.

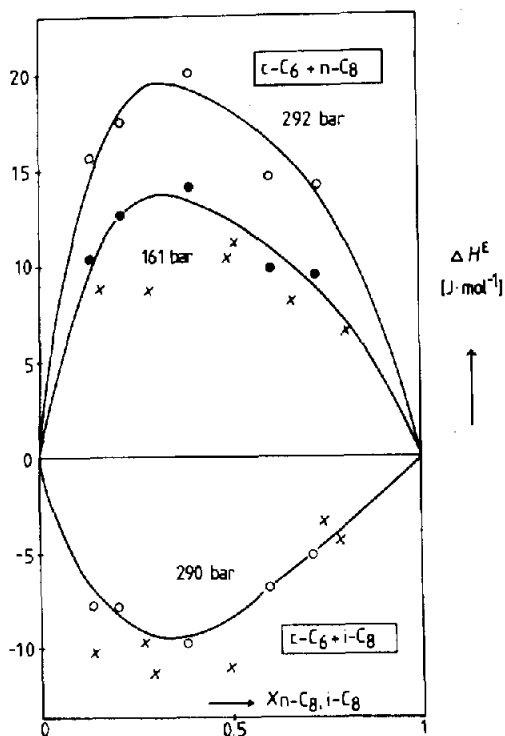


Fig. 6. Effect of pressure on the composition dependence of H^E for $c\text{-C}_6 + n\text{-C}_8$ and $c\text{-C}_6 + i\text{-C}_8$ at 298.15 K. o, ● measured; — Redlich-Kister fit; x determined indirectly from excess volumes using equation (4) (at 161 bar for the $n\text{-C}_8$ mixture and at 290 bar for $i\text{-C}_8$ mixture).

According to the exact thermodynamic relation

$$\left(\frac{\partial H^E}{\partial p}\right)_T = V^E(p) - T\left(\frac{\partial V^E}{\partial T}\right)_p \quad (4)$$

at a given temperature the variation of H^E with pressure and composition can be calculated indirectly from the dependence of V^E on pressure, temperature and composition. One way to determine V^E is to measure densities of mixtures and pure components at various pressures and temperatures. Those measurements, however, have to

be extremely accurate, as for liquid mixtures V^E in general is pretty small. Using a vibrating-tube densitometer (e.g. DMA 601, Paar/Heraeus) at ambient pressure and a bellows-dilatometer at high pressures those measurements are possible (ref. 19, 20) and the excess volume is obtained according to:

$$V^E = \frac{M_A x_A + M_B x_B}{\rho_M} - x_A \cdot \frac{M_A}{\rho_A} - x_B \cdot \frac{M_B}{\rho_B} \quad (5)$$

where M_A and M_B are the molar masses, x_A and x_B are the mole fractions and ρ_A and ρ_B are the densities of the components A and B respectively. ρ_M is the density of the mixture.

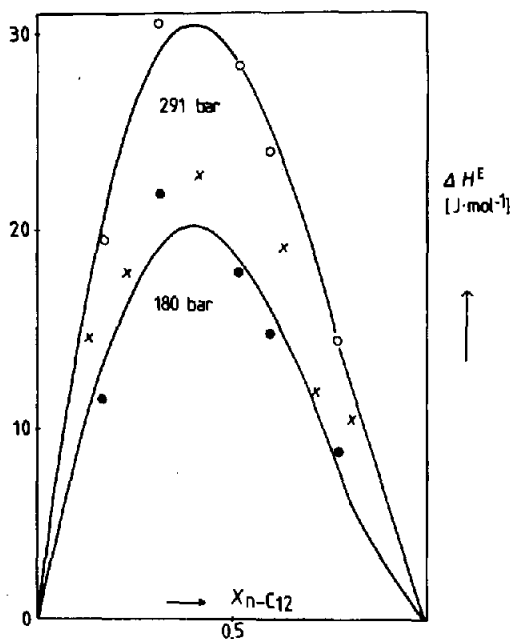


Fig. 7. Effect of pressure on the composition dependence of H^E for $c\text{-C}_6 + n\text{-C}_{12}$ at 298.15 K. o, ● measured; — Redlich-Kister fit; x determined indirectly at 180 bar from excess volumes using equation (4).

For all mixtures discussed by Heintz et al. (ref. 18) V^E -data have been obtained in this way at various temperatures and ambient pressure. The slope $(\partial V^E/\partial T)_p = 1$ bar was determined at 298.15 K and the corresponding ΔH^E -values for a given Δp were calculated using equation (4). The results are included in Figs. 6 - 8 and are marked as determined indirectly. The V^E -data are accurate to within 2 - 3%,

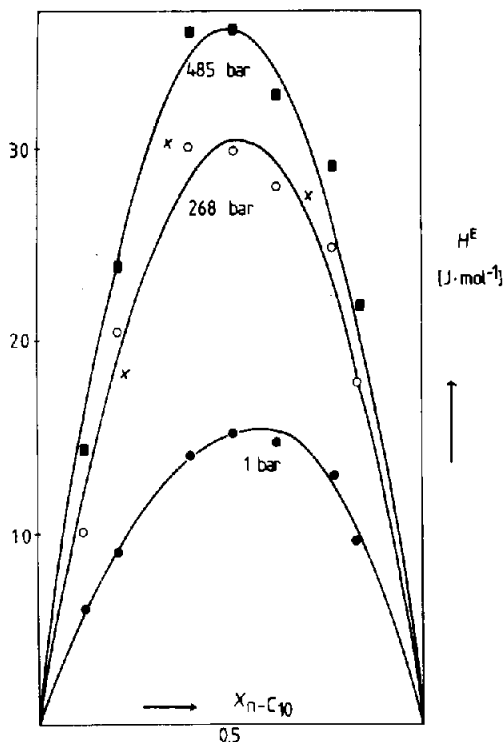


Fig. 8. Composition dependence of H^E at various pressures and 298.15 K for $n\text{-C}_6 + n\text{-C}_{10}$. o, ●, measured; — Redlich-Kister fit; x determined indirectly at 268 bar from excess volumes using equation (2).

but the temperature dependence of V^E is very small and hence relatively inaccurate. In calculating $(\Delta H^E/\Delta p)$ from equation (4) that is important as $(\partial V^E/\partial T)_p$ is multiplied by T , i.e. by a relatively large number. Therefore, the indirectly determined ΔH^E -values are only accurate to within $\pm 25\%$ (with respect of the absolute H^E -

values that means about $\pm 2\%$), possible systematic errors not included. This error is nearly twice as high as the one of the ΔH^E -values measured directly with the flow calorimeter, which are estimated to be accurate at least to within $\pm 1.5\%$ of the H^E -values involved. Within those experimental errors the ΔH^E -values obtained in the different ways agree with each other and hence the data are thermodynamically consistent.

Theoretical Interpretation

Thermodynamic excess properties of liquid mixtures containing molecules of different size and shape (especially chain-molecules) have been discussed on the basis of molecular statistics very successfully using the Prigogine-Flory-Patterson free volume theory (PFP-Theory) (ref. 21-24). The theoretical equations derived from this theory to describe the dependence of the excess properties on temperature, pressure and composition contain quite a number of system specific parameters. However, for a binary mixture all these parameters, except one, can be calculated from pure component data (e.g. p,V,T-data). The so-called interaction parameter X_{12} remains the only one being adjustable to represent the excess properties properly. This parameter is related to the difference of the different intermolecular interactions between different molecules. As a molecular parameter it is regarded to be independent of temperature, pressure and composition.

For a large number of liquid mixtures, in particular for polymer solutions, the PFP-Theory predicts good results for the thermodynamic excess properties after the parameter X_{12} has been adjusted properly (e.g. using an experimental value of H^E). In some cases, however, inconsistencies of the theory have been observed for various reasons. For mixtures of n-alkanes with relatively compact (globular) molecules (e.g. c-C₆) X_{12} shows a significant decrease with increasing temperature (ref. 25). This is incompatible with the concepts of the PFP-Theory, which regards X_{12} being independent of temperature. Furthermore the X_{12} -values determined from H^E -data for mixtures of c-C₁₆ + n-alkanes are much larger than those obtained

for mixtures of $c\text{-C}_6$ with the corresponding branched isomers (ref. 25). The same results are obtained from experimental data of the excess volume (ref. 19). This fact cannot be explained by the different numbers of methyl- and methylene-contacts within the different mixtures of the different isomers, as the difference in the intermolecular interaction energy is too small. Additionally for mixtures of $c\text{-C}_6$ + n -alkanes X_{12} was found to increase with increasing pressure, when determined from H^E -data at various pressures (ref. 26). Again this is incompatible with the concepts of the PFP-Theory which regards X_{12} being independent of pressure. For mixtures of $c\text{-C}_{16}$ with corresponding isomers such a pressure dependence was not observed.

Figs. 9 and 10 show for the mixtures $c\text{-C}_6$ + $n\text{-C}_8$ and $c\text{-C}_6$ + $n\text{-C}_{12}$ the experimental and calculated results for the differences ΔH^E .

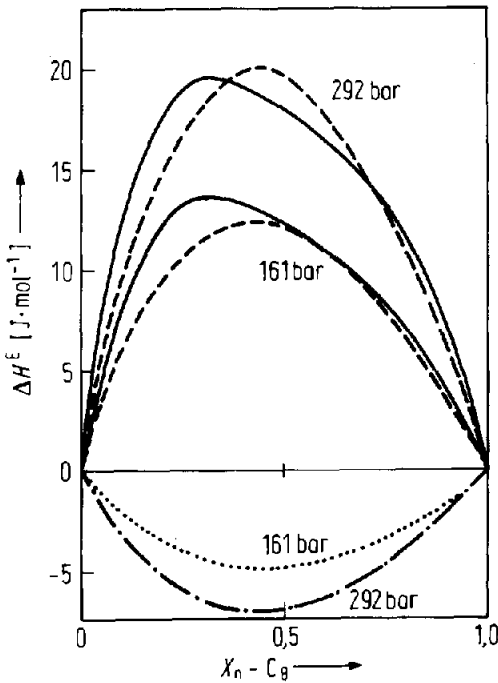


Fig. 9. Effect of pressure on the composition dependence of H^E for $c\text{-C}_6$ + $c\text{-C}_8$ at 298.15 K. — experiment (Redlich-Kister fit); ---- PFP-Theory with $X_{12}(p)$; -.-.-, PFP-Theory with $X_{12}(1 \text{ bar})$.

Within the error of the experimental data (see ref. 18) the agreement is very good. The calculations with the PFP-Theory are very sensitive to small changes in X_{12} . If at high pressures, for example, the calculations are performed using the same X_{12} as at 1 bar for all $c\text{-C}_6 + n\text{-alkane}$ systems much too small ΔH^E -values are obtained, even negative ΔH^E -values are predicted as shown in Figs. 8 and 9.

The origin of these discrepancies has first been recognized by depolarized light scattering performed with pure n -alkanes and their mixtures with $c\text{-C}_6$ (see e.g. ref. 27). According to these results within liquid n -alkanes exists some short range order which is destroyed upon mixing with a compact molecule like $c\text{-C}_6$. This molecular order most probably can be interpreted as a packing effect favoured between segments of different n -alkane chains. Apparently this is associated with an energetic stabilisation in relation to the completely desoriented state. Upon mixing with $c\text{-C}_6$ this short range order is destroyed gradually, depending on the composition of the mixture. The associated energy leads to a larger endothermic excess enthalpy and hence to a larger X_{12} -value. The decrease of X_{12} with increasing temperature shows that the short range order within the pure n -alkanes already is partially destroyed by thermal motion before mixing. These effects are small or do not exist at all for mixtures containing the branched isomeric alkanes, as these pure components show only little or no short range order due to steric hinderance (ref. 25). Along the same lines the increase of X_{12} with increasing pressure is physically reasonable as at higher pressures the short range order is expected to be more distinct, thus leading to a larger endothermic excess enthalpy and hence to a larger X_{12} -value. Again these effects of pressure are small or do not exist at all for mixtures containing branched isomeric alkanes (X_{12} for $c\text{-C}_6 + i\text{-C}_8$ is independent of pressure).

Making use of these qualitative results the PFP-Theory has been modified and extended quantitatively in order to take into account possible short range order present in liquids (ref. 26). Within the framework of the extended PFP-Theory X_{12} is depending on temperature and pressure according to the following relation:

$$X_{12} = X_{12}^0 \cdot \frac{T}{T - T_0(p)} \quad (T > T_0) \quad (6)$$

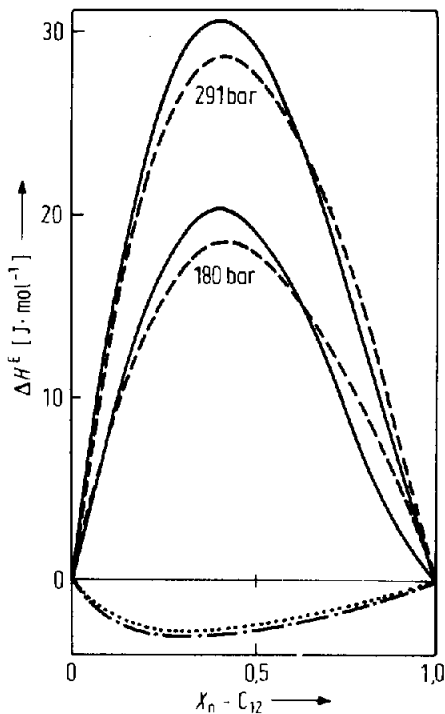


Fig. 10. Effect of pressure on the composition dependence of H^E for $c\text{-C}_6 + n\text{-C}_{12}$ at 298.15 K. — experiment (Redlich-Kister fit); ---- PFP-Theory with $X_{12}(p)$; -.-.-, PFP-Theory with $X_{12}(1 \text{ bar})$.

X_{12}^0 is the interaction parameter in case no short range order is present and hence it is independent of temperature and pressure. $T_0(p)$ formally has the significance of a transition temperature, which for a given pressure can be determined together with X_{12}^0 from the temperature dependence of X_{12} . At 1 bar T_0 was found to be lower than the melting temperature T_m (ref. 25) and in fact transition phenomena have been observed for some alkanes below T_m (ref. 28).

The pseudo-transition temperature $T_0(p)$ should increase with increasing pressure as at higher densities the short range order is more distinct and that is in fact the case for mixtures of $c\text{-C}_6 +$

n-alkanes (ref. 26). The origin for the increasing X_{12} with increasing pressure hence is the increase of $T_0(p)$. An averaged increase of 8 K was obtained for an increase in pressure of 300 bar. It is interesting to compare this number with the results obtained by Würflinger (ref. 28), who measured the pressure dependence of the transition temperature in the solid state for some alkanes using the DTA-method. He found an increase of 5 - 10 K for an increase in pressure of 300 bar. This agreement is somewhat surprising, as Würflinger not only has investigated n-alkanes but also more globular molecules, which show the typical rotational transition of practically first order. The processes characterized by $T_0(p)$, however, are occurring within a wider temperature range. Nevertheless the direct investigations of transitions and their dependence on pressure support the physical interpretation and the theoretical concept of short range order within liquid n-alkanes.

The extended PFP-Theory discussed accounts for possible short range order present in liquids. Such order, for example, exists within n-alkanes and hence only the PFP-Theory in its extended form gives a consistent description of the temperature and pressure dependence of H^E of the alkane mixtures discussed here. The results clearly indicate that very reliable H^E -data over a wide pressure and temperature range make possible a rigorous test of molecular theories of fluids and their mixtures.

ALCOHOL + ALKANE MIXTURES

For such mixtures the thermodynamic excess properties depend mainly on the association due to hydrogen bonding of the alcohol. As the temperature dependence of the excess properties gives some information about the enthalpy of hydrogen bonding, the pressure dependence should give some insight in the volume change associated with the formation of hydrogen bonds.

Experimental Results

H^E -data at high pressures have only been reported by Heintz (ref. 30)

and more recently by Oswald (ref. 31). Fig. 11 shows results for the mixture 2-propanol + n-heptane experimental at various pressures and temperatures (from ref. 30). An increase of H^E with increasing temperature and a decrease with increasing pressure is obtained. The alcohol + alkane mixtures show a dependence on pressure and temperature which is opposite to the one for alkane + alkane mixtures. From a physical point of view this is the important result.

Hess has determined the pressure dependence of H^E from his V^E -data using equation (4) (ref. 29). For an equimolar mixture of 2-propanol + n-heptane at 298.15 K Fig. 12 shows a comparison of the pressure dependence of H^E as determined directly with the calorimeter by Heintz (ref. 30) and indirectly by Hess. The results obtained in the different ways agree well showing the V^E -data and H^E -data to be thermodynamically consistent.

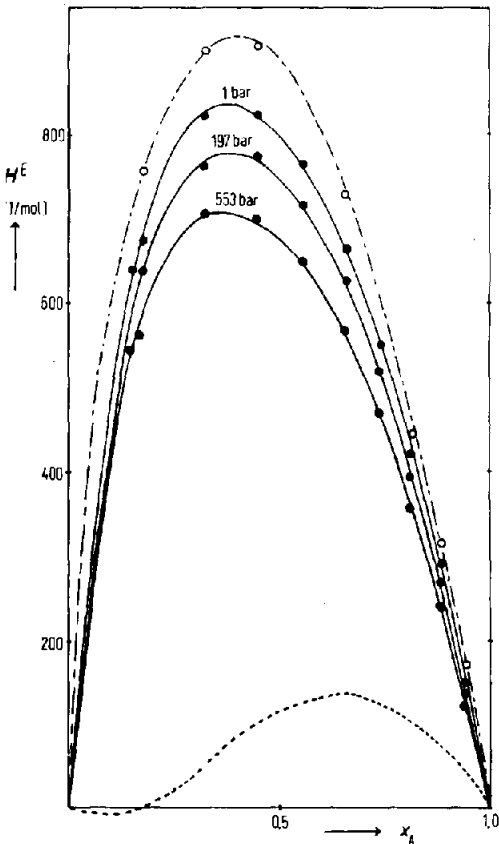


Fig. 11. Composition dependence of H^E at various temperatures

and pressures for 2-propanol + n-heptane. ● measured at 298.15 K and pressures indicated; ○ measured at 303 K and 1 bar; — Redlich-Kister fit; $H_{\text{phys.}}^E = H_{\text{exp.}}^E - H_{\text{chem.}}^E$ according to equation (7).

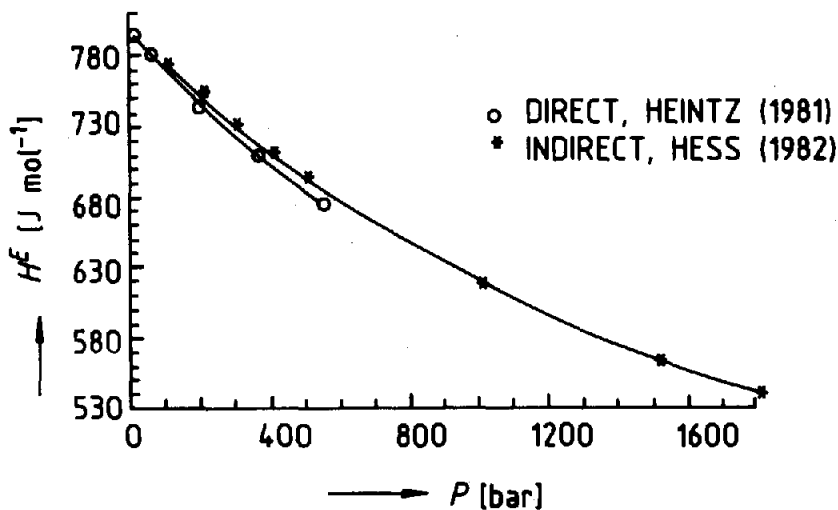


Fig. 12. Pressure dependence of H^E for an equimolar mixture of 2-propanol + n-heptane at 298.15 K. ○ (ref. 30) and * (ref. 29) measured; — best fit.

Theoretical Interpretation

In case of mixtures with associating components like alcohols mostly quasi rigid lattice theories have been applied, based on real association models (ref. 32, 33) or approaches like UNIFAC (ref. 34). These theories are very useful for a systematic description of the Gibbs excess energy G^E and H^E but they neglect all excess properties related to V^E , $(\partial V^E/\partial p)_T$ or $(\partial H^E/\partial T)_p$ as $V^E = 0$ is assumed. The real association solution model, for example, has been applied

successfully to mixtures with strong hydrogen bonding components like alcohols. In this theory thermodynamic properties are split in a so-called chemical and physical contribution (e.g. $H^E = H_{\text{chem}}^E + H_{\text{phys}}^E$). At low pressures the model allows a consistent description of G^E and H^E (ref. 33, 35). The model assumes that linear i-mers of associated alcohol molecules are formed by consecutive "chemical reaction" (ref. 32, 35). The final equation for H^E at normal pressure is obtained as follows:

$$H^E = \Delta h_0 \cdot K \cdot (\theta_1 - \theta_1^0) \cdot x_A + B' \theta_A \cdot (1 - \theta_A) \quad (7)$$

where the first term represents H_{chem}^E and the second one H_{phys}^E . Δh_0 is the enthalpy of formation of hydrogen bonds and x_A is the mole fraction of alcohol. θ_1 and θ_1^0 are the volume fractions of alcohol monomers in the solution and the pure alcohol respectively, depending only on the association konstant K and x_A . K is regarded as independent of the number i of associated units, an assumption being justified by Flory (ref. 37). θ_A is the volume fraction of alcohol. B' is related to the differences in the intermolecular interactions between the different molecules of the mixture.

Renon and Prausnitz (ref. 33) found $\Delta h_0 = -25.1 \text{ kJ mol}^{-1}$, being the same for different alcohol + hydrocarbon systems. For 2-propanol + n-heptane $K = 60$ was found at 323 K. With these values the H^E -data for this mixture at 298.15 K and 1 bar can be described well using the following equation for the temperature dependence of K :

$$\left(\frac{\partial \ln K}{\partial T}\right)_p = + \frac{\Delta h_0}{RT^2} \quad (8)$$

In this way at 298.15 K a value of $K = 131.5$ was obtained. The value for H_{phys}^E calculated by taking the difference $H_{\text{exp}}^E - H_{\text{chem}}^E$ is shown in Fig. 7. At its maximum H_{phys}^E is 140 J mol^{-1} (for $x_A = 0.65$) and for low alcohol compositions it has even small negative values. With increasing pressure H_{phys}^E decreases slightly.

The real associated solution model shows that hydrogen bonding accounts for the main contribution to H^E also at higher pressures.

This result was not only found for the 2-propanol + n-heptane system discussed but also for other alcohol + alkane systems (ref. 30, 31). As the model is not able to describe V^E and related properties like $(\partial H^E/\partial p)_T$ Heintz (ref. 30) has extended the theory in order to account for the volume change associated with the formation of hydrogen bonds. To a first approximation the different numbers of hydrogen bonds in solution and in the pure alcohol are calculated using the same kind of equation for V_{chem}^E , as for H_{chem}^E :

$$V_{chem}^E = \Delta v_o \cdot K \cdot (\phi_1 - \phi_1^0) \cdot x_A \quad (9)$$

Here Δv_o is the volume change associated with the formation of one mol hydrogen bonds; the notations x_A , K , ϕ_1 and ϕ_1^0 meaning the same as before. From the values reported in literature (ref. 38) $v_o = -4 \text{ cm}^3 \cdot \text{mol}^{-1}$ has been chosen as the most probable one. V_{chem}^E calculated with equation (9) for the maximum of the V^E versus composition plot gives $0.12 \text{ cm}^3 \text{ mol}^{-1}$ for 2-propanol + n-heptane in contrast to the experimental value found to be $0.60 \text{ cm}^3 \text{ mol}^{-1}$ (ref. 39). The resulting value for the physical contribution is $V_{phys}^E = 0.48 \text{ cm}^3 \text{ mol}^{-1}$ clearly shows that this contribution is dominating.

In calculating H_{chem}^E at high pressures the product $p \cdot V_{chem}^E$ has to be added to the first term in equation (7) with V_{chem}^E given by equation (9). The value of K at high pressures is obtained using the relation:

$$\left(\frac{\partial \ln K}{\partial p}\right)_T = -\frac{\Delta v_o}{RT} \quad (10)$$

The results obtained for $\Delta H_{chem}^E = H_{chem}^E(p) - H_{chem}^E(1 \text{ bar})$ in this way are shown in Figs. 13 and 14 for the mixtures 2-propanol + n-heptane and 2-propanol + i-C₈ respectively. In both cases the chemical contribution is about 20% of the total value of $(\Delta H^E/\Delta p)_T$ determined experimentally. Again, as already found for V^E , the physical contribution is larger than the chemical one.

In conclusion it follows that in mixtures of alcohol + alkane the physical contribution according to the real associated solution model plays a more important role than the chemical one for those

excess properties which are associated with V^E . This already has been suggested by Treszczanowicz and Benson (ref. 40) in the interpretation of their V^E -data of alcohol + hydrocarbon mixtures. Directly measured H^E -data at high pressures confirm this conclusion as discussed here.

High pressure thermodynamic properties depend the stronger on the change of volume the higher the pressure is. To obtain better description at such important state conditions the extended real associated solution model provides a reasonable basis for further theoretical work. Most important are efforts to develop a theoretical expression for the physical contribution of excess properties including the change in free volume. This would allow a better physical insight in the dependence of the excess properties of associated systems on pressure.

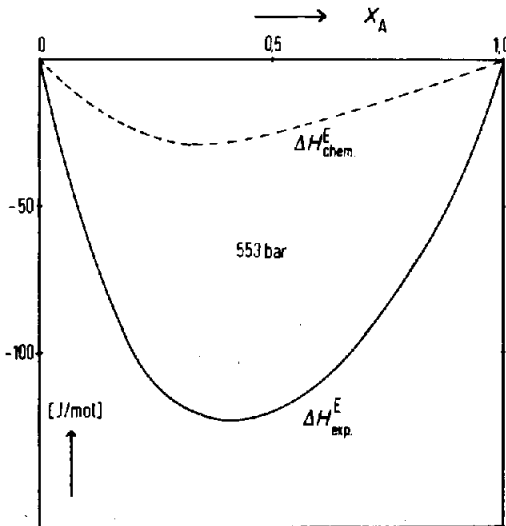


Fig. 13. Effect of pressure on the composition dependence of H^E for 2-propanol + n-heptane at 298.15 K. — experiment (Redlich-Kister fit): $\Delta H^E_{exp} = H^E(p) - H^E(1 \text{ bar})$; ----- according to equations (7) and (9).

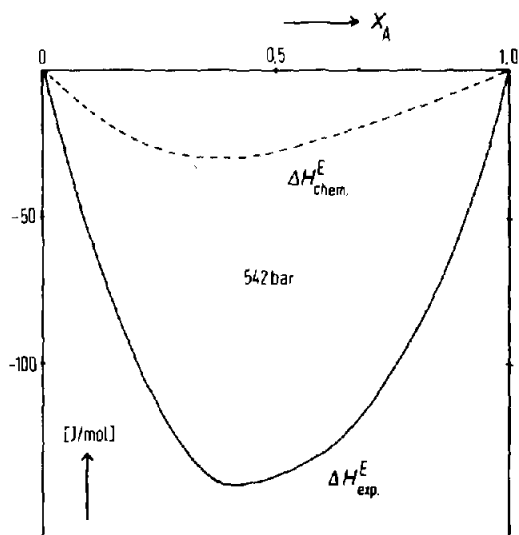


Fig. 14. Effect of pressure on the composition dependence of H^E for 2-propanol + 2,2,4-trimethylpentane (i-C₈) at 298.15 K
 — experiment (Redlich-Kister fit): $\Delta H^E_{exp.} = H^E(p) - H^E(1 \text{ bar})$; ---- according to equations (7) and (9).

REFERENCES

- 1 Engels, P. and Schneider, G.M., 1972, Ber. Bunsenges. Phys. Chem., 76: 1239 - 1242.
- 2 Götze, G. and Jeschke, P., 1977, Ber. Bunsenges. Phys. Chem., 81: 933 - 936.
- 3 Jeschke, P. and Schneider, G.M., 1978, J. Chem. Thermodynamics, 10: 803 - 808.
- 4 Dymond, J.H., Young, K.J. and Isdale, J.D., 1979, J. Chem. Thermodynamics, 11: 887 - 895.
- 5 Ohling, W. and Schneider, G.M., 1979, J. Chem. Thermodynamics, 11: 305 - 306.

- 6 Götze, G. and Schneider, G.M., 1980, *J. Chem. Thermodynamics*, 12: 661 - 672.
- 7 Seward, T.M. and Franck, E.U., 1981, *Ber. Bunsenges. Phys. Chem.*, 85: 2 - 7.
- 8 Nunes da Ponte, M., Streett, W.B. and Stavely, L.A.K., 1978, *J. Chem. Thermodynamics*, 10: 151 - 168.
- 9 Lee, J.I. and Mather, A.E., 1970, *J. Chem. Thermodynamics*, 2: 881 - 895.
- 10 Wormald, C.J., Lewis, K.L. and Mosedale, S., 1977, *J. Chem. Thermodynamics*, 9: 27 - 42.
- 11 Bier, K., Kunze, J. and Maurer, G., 1980, *J. Chem. Thermodynamics*, 12: 137 - 164.
- 12 Christensen, J.J., Izatt, R.M., Eatough, D.J. and Hansen, L.D. 1978, *J. Chem. Thermodynamics* 10: 25 - 34.
- 13 Lentz, H., 1977, *Ber. Bunsenges. Phys. Chem.*, 81: 1073 - 1076.
- 14 Heintz, A. and Lichtenthaler, R.N., 1979, *Ber. Bunsenges. Phys. Chem.*, 83: 853 - 856.
- 15 Christensen, J.J., Hansen, L.D., Izatt, R.M., Eatough, D.J. and Hart, R.M., 1981, *Rev. Sci. Instrum.*, 52: 1226 - 1231.
- 16 Siddiqi, M.A. and Lucas, K., 1982, *J. Chem. Thermodynamics*, 14: 1183 - 1190.
- 17 Christensen, J.J., Hanks, R.W. and Izatt, R.M., 1982, "Handbook of Heats of Mixing", J. Wiley and Sons, New York.
- 18 Heintz, A. and Lichtenthaler, R.N., 1980, *Ber. Bunsenges. Phys. Chem.*, 84: 727 - 732.
- 19 Heintz, A., 1979, *Ber. Bunsenges. Phys. Chem.*, 83: 155 - 160.
- 20 Bazúa, E.R., EBwein, D. and Lichtenthaler, R.N., 1983, *Ber. Bunsenges. Phys. Chem.*, 87: in press.
- 21 Prigogine, I., 1957, "The Molecular Theory of Solutions", North Holland Corp., Amsterdam.
- 22 Flory, P.J., Orwoll, R.A. and Vrij, A., 1964, *J. Am. Chem. Soc.*, 86: 3507 - 3520.

- 3 Patterson, D. and Delmas, G., 1970, Discuss. Faraday Soc., 49: 98 - 105.
- 4 Eichinger, B.E. and Flory, P.J., 1968, Trans. Faraday Soc., 64: 2035 - 2052.
- 5 Heintz, A. and Lichtenthaler, R.N., 1977, Ber. Bunsenges. Phys. Chem., 81: 921 - 925.
- 6 Heintz, A. and Lichtenthaler, R.N., 1980, Ber. Bunsenges. Phys. Chem., 84: 890 - 895.
- 7 Tancrède, P., Bothorel, P., St. Romain, P. de and Patterson, D., 1977, J. Chem. Soc., Faraday Trans. 2, 73: 15 - 39.
- 8 Würflinger, A., 1975, Ber. Bunsenges. Phys. Chem., 79: 1195 - 1201
- 9 Hess, D., 1982, Diploma-Thesis, Abteilung für Chemie, Ruhr-Universität Bochum, 4630 Bochum 1, West Germany.
- 0 Heintz, A., 1981, Ber. Bunsenges. Phys. Chem., 85: 632 - 635.
- 1 Oswald, G., 1982, Diploma-Thesis, Physikalisch-Chemisches Institut, Universität Heidelberg, 6900 Heidelberg 1, West Germany.
- 2 Kretschmer, C.B. and Wiebe, R., 1954, J. Chem. Phys., 22: 1697 - 1701.
- 3 Renon, H. and Prausnitz, J.M., 1967, Chem. Eng. Sci., 22: 299 - 309; Errata: 1891 - 1892.
- 4 Fredenslund, A., Gmehling, J. and Rasmussen, P., 1977, "Vapour-Liquid Equilibria Using UNIFAC", Elsevier, Amsterdam.
- 5 Nagata, I., 1973, Z. Phys. Chem. (Leipzig), 252: 305 - 311.
- 6 Kehiaian, H. and Treszczanowicz, A., 1969, Bull. Soc. Chim. Fr., 18: 1561 - 1577.
- 7 Flory, P.J., 1944, J. Chem. Phys., 12: 425 - 438.
- 8 Josefiak, C. and Schneider, G.M., J. Phys. Chem., 84: 3004 - 3007.
- 9 Ness, H.C. van, Soczek, C.A., Peloquin, G.L. and Machado, R.L., 1967, J. Chem. Eng. Data, 12: 217 - 223.
- 0 Treszczanowicz, A.J. and Benson, G.C., 1978, J. Chem. Thermodynamics, 10: 967 - 974.